ULTRASTRUCTURAL AND MOLECULAR CHARACTERISTICS OF CRAYFISH PHOTORECEPTOR MEMBRANES

HECTOR R. FERNANDEZ and ELVIRA E. NICKEL. From the Department of Biological Sciences, University of Southern California, Los Angeles, California 90007, and the Department of Biology, University of Konstanz, Konstanz D 775, West Germany

Reports on the molecular characteristics of vertebrate photoreceptor membranes have appeared recently (1, 7, 16, 21). Among invertebrates, some of the fundamental functional and anatomical properties of crayfish photoreceptors have also been studied (9–13, 17, 24–26, 29, 35, 36, 38, 39), but little is known about their molecular properties. This paper presents recent freeze-fracture and thin section investigations on the relation between crayfish photoreceptor membranes and their molecular characteristics.

MATERIALS AND METHODS

Light- and dark-adapted specimens of the crayfish *Procambarus clarkii* (Girard) were used. Dark-adapted retinas (12–18 h) were dissected in dim red light of 700 nm (Balzers B-40 interference filter, Rolyn Optics, Arcadia, Calif.). For ultrastructural studies, whole ret-

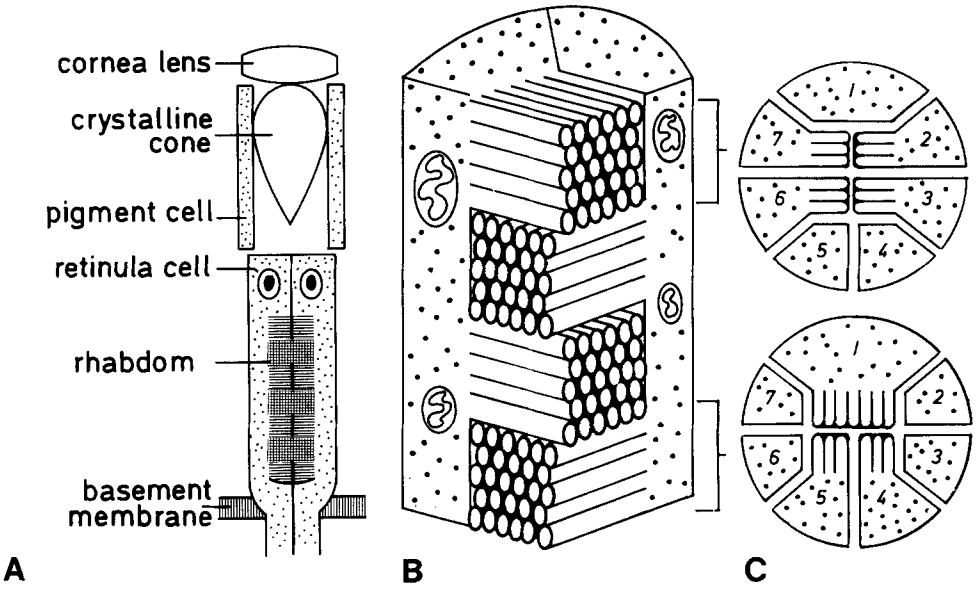

FIGURE 1 Diagrams of an ommatidium from the compound eye of *P. clarkii*. (A) Longitudinal section through the optic axis. The retinula cells form a fused rhabdom which consists of 20–25 layers of closely packed microvilli. (B) Stereodiagram of parts of two retinula cells and several layers of orthogonally oriented microvilli. (C) Cross sections through the retinula. They show the contribution of the retinula cells to alternate layers of microvilli (diagrams after Eguchi [9] and Eguchi and Waterman [10]).

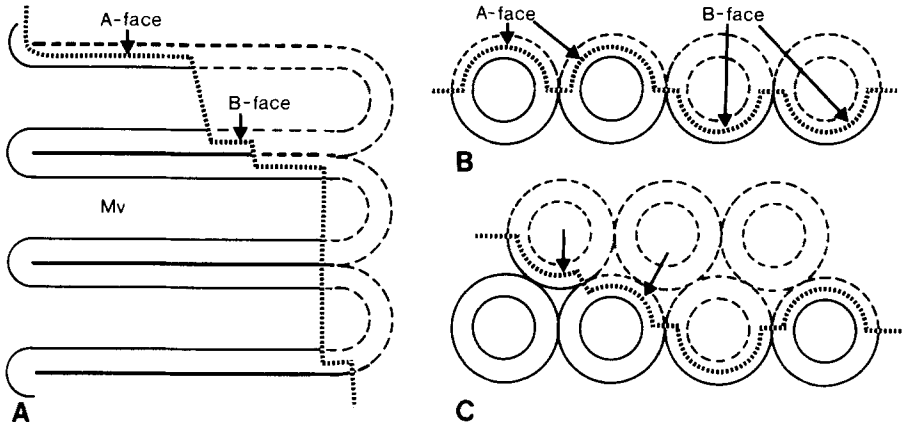

FIGURE 2 Schematic drawings of fracture planes (dotted lines) that account for most of the observed fractures through the microvilli. Under the assumption that freezing weakens hydrophobic bonds, the fracture occurs along a plane within the membrane itself. The cleaving separates the two lipid layers, thus exposing two fracture faces inside the membrane (2, 8, 28). These two faces are called, according to the nomenclature of McNutt and Weinstein (22), the A face (cytoplasmic side = convex) and B face (extracellular side = concave). True surfaces of the membranes are not revealed by fracturing. The interrupted lines indicate the tissue which has been removed by fracturing. The solid lines represent the replicated membrane faces. (A) Fractures parallel and perpendicular to the longitudinal axis of microvilli (*Mv*), revealing A and B faces of the membrane. (B) Fracture planes which explain alternating convex and concave profiles of microvilli. (C) Fracture planes which produce incomplete faces of microvilli (arrows). Since the fractures actually occur through three-dimensional structures, the interpretation of many fractures presented in the illustrations requires a combination of these diagrams.

inas or fragments were prefixed in 3% (vol/vol) glutaraldehyde in crustacean Ringer's (pH 7.4) (33) for 1 h at 4°C. Corneas, lenses, and crystalline cones were removed to allow better penetration of the fixative. After rinsing with Sorenson's buffer (0.06 M, pH 7.4), fixation in 1% OsO_4 (same buffer and pH), and dehydration in graded concentrations of acetone, specimens were embedded in Araldite. Thin sections were cut with a Reichert Om U2 microtome (American Optical Corp., Scientific Instrument Div., Buffalo, N.Y.) and stained with either lead citrate (34) or 4% aqueous uranyl acetate.

For freeze-fracturing, small blocks of prefixed retinas were impregnated in 30% (vol/vol) glycerol in crustacean Ringer's for 30–40 min. Tissue samples were placed on gold disks, frozen in liquid Freon R22 (Dupont Instruments, Wilmington, Del.), and further processed according to the method of Moor et al. (23) in a Balzers freeze-etch device BA 360M (Balzers High Vacuum Corp., Santa Ana, Calif.). Replicas were obtained by shadowing the cleaved surfaces with carbon-platinum. Tissues were removed by digestion in 40% chromic acid, and after rinsing in distilled water the replicas were placed on coated grids. Electron micrographs of the replicas represent positive images in which the shadows appear light and the structural profiles as dark platinum deposits. Large arrows in the micrographs indicate the direction of the platinum shadowing.

The effect of digitonin on the ultrastructure of photoreceptor membranes was investigated by treating small fragments of dark-adapted retinas with 1% (wt/vol) digitonin (Fisher Scientific Co., Fair Lawn, N. J.) in Ringer's for periods of 5, 10, and 15 min at 1°C in the dark. Then the tissue was processed as described above. All samples were examined with a Zeiss EM 10 electron microscope at 80 kV with a 50-μm objective aperture. An anticontamination cooling device was used routinely.

The measurement of particle diameter was carried out on 62,000 × negative film by selecting areas of 0.6 cm^2 which lie along a diagonal line between two opposite corners of the negative. A 12 × binocular microscope and an ocular micrometer with a 0.1-mm scale were used. The diameter of a particle is defined as the length of the base of its triangular shadow. Particles were selected which lie in an axis parallel to the direction of shadowing and in an axis perpendicular to it.

RESULTS

In *Procambarus*, the structural units of the compound eye, the ommatidium, contains seven receptor (retinula) cells (9, 10, 11); a rudimentary eighth cell recently found in *Astacus* (17) has not been reported for *Procambarus*. The rhabdom is formed by tubular evaginations (microvilli) of the retinula cell membrane, and it is in these membranes that the photopigment molecules are located (39). Structural details of the rhabdom are shown in Fig. 1. In thin sections the microvilli have a diameter of 0.08 μm and a length of 10 μm (Figs. 3 and 4). The diagrams in Fig. 2 illustrate our interpretation of the observed fracture planes through the microvilli. Fig. 5, a tangential fracture through the retina, shows a retinula cell and an adjacent pigment cell with convex and concave profiles of pigment granules. The A face of the receptor cell membrane is revealed in an area from which microvilli arise. Craterlike structures on this A face are the sites where microvilli have been broken away. Between the craters, the membrane is covered by randomly distributed particles; there are about 900 particles/μm^2 with a mean diameter of 80 Å.

In Fig. 6 A, the fracture plane runs through two adjacent layers of microvilli. B faces of longitudinally fractured microvilli appear as concave smooth profiles. The upper part of the picture shows convex A faces of microvilli which are covered by particles, while, on the right side, granular A faces of microvilli alternate with smooth B faces. The extent to which a microvillus is exposed by the freeze-cleaving process varies considerably.

Alternating A and B faces of microvilli are shown in Fig. 6 B at higher magnification. Usually, in both light- and dark-adapted retinas, the particles appear to be randomly distributed on the A faces of the microvilli membranes. However, small membrane areas appear occasionally in which particles are arranged in diagonal rows (Fig. 6 B, *inset*). This ordered distribution was found in different rhabdomeres and could not be associated with microvilli of a particular retinula cell. Since such particle arrangement was found in light- and dark-adapted retinas, it is not yet clear what its significance is.

Accurate estimates of particle size must take into account the convexity of the A faces of the microvilli, and the varying location of the particles with respect to the direction of shadowing. In the plane of the membrane, the diameter of the particles ranged from 50 to 275 Å and had a mean value of 84 Å (Fig. 7). There are about 6,600 particles/μm^2 of membrane surface. The B faces appear rather smooth except for a few scattered pits. The pits were recognized by their inverted shadows with respect to those of the particles (Fig. 6 B, *inset*, arrows). These pits probably represent the sites where some of the larger particles observed on the A faces extend into the outer lipid layer. Cross-fractured microvilli at high magnification (Fig. 6 C) reveal the two membrane layers

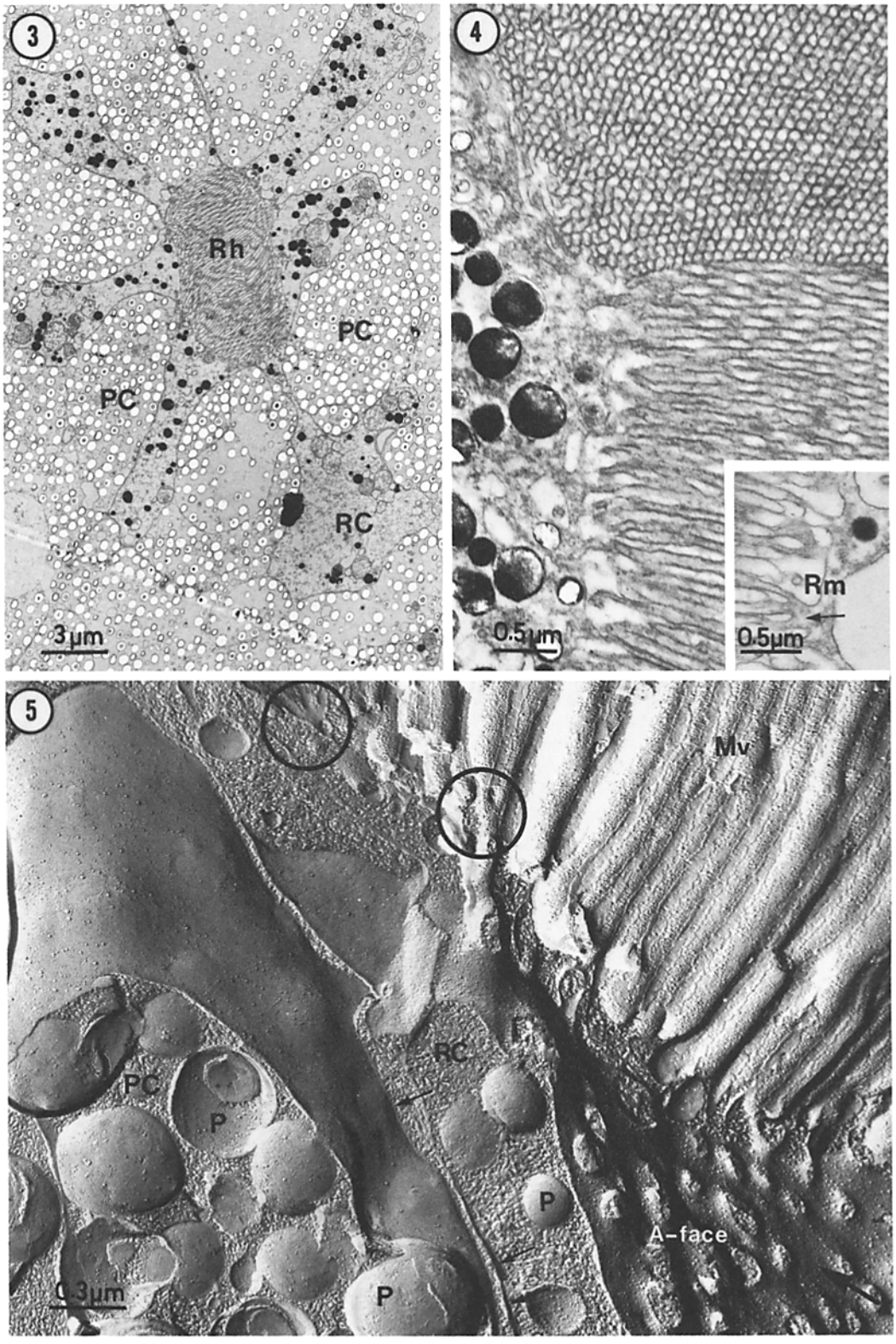
3
Rh
PC
PC
RC
3μm
4
0.5μm
Rm
0.5μm
5
Mv
RC
PC
P
P
P
A-face
0.3μm

and the associated particles on the inner membrane face. The mean transmembrane particle diameter was 80 Å and had a similar range of values. Thus, it seems that the particles are spherical in shape. There are 16–20 particles around the microvillus circumference. No difference in the particle distribution was found when light- and dark-adapted retinas were compared.

There have been recent reports of electrical coupling between retinula cells in crayfish compound eyes (24). A search for morphological clues of the coupling was made, particularly in the region where the ends of opposing microvilli meet in the middle of each layer. The A and B faces at the ends of microvilli appear similar to corresponding faces in other parts of the microvilli. No special membrane structures were observed which would support the assumption that electrical coupling occurs via the tips of opposing microvilli. (See also Perrelet et al. (27), Plate III, Fig. d).

Effect of Digitonin

Thin sections and freeze-fracture replicas of retinal tissues treated with digitonin show drastic changes in the ultrastructure of the microvilli (Figs. 8 and 9). The typical hexagonal arrangement of the microvilli within each layer is disturbed. Very often, the microvilli appear swollen. They also break into small fragments, forming multilayered structures or aggregates within the rhabdom or in the retinula cell cytoplasm. Freeze-fracture replicas show a second effect. The particles on the A faces of untreated microvilli are gradually removed by digitonin treatment. In disrupted microvilli, which still maintain a more or less parallel orientation (Figs. 9 A and B), a few particles still remain attached to the A faces. In smaller aggregates, the particles are completely absent (Fig. 9C). Comparison of tissues which have been treated with digitonin for various lengths of time shows that all stages of the digitonin effect are seen, irrespective of the length of treatment. The effect usually is most extensive in the periphery of the rhabdom and, with increased length of treatment, progresses inwardly.

DISCUSSION

Freeze-fracture replicas of crayfish microvilli show particles associated with the A face of the membrane while the B face appears smooth. The mean diameter of the spherical particles is about 80 Å, their mean density 6,600 μm^2. These observations are in basic agreement with published freeze-fracture studies of the rhabdom of the honey bee (27). Even though comparable measurements were not reported for the honey bee, inspection of the published electron micrographs suggests that the particle density is similar. The questions which immediately arise are: what is the nature of these particles and what can be said of their disposition in the receptor membrane?

Usually, the particles have a random orientation. However, occasionally they appear arranged in rows, and the rows are oriented diagonally with respect to the longitudinal axis of the microvillus (Fig. 6 B, *inset*). In rows with the densest packing of particles, the smallest center-to-center distance measures about 85 Å, which is in good agreement with the calculations of Hamdorf and Schwemer (14) and of Liebman (19).

The B faces of the microvilli do not show depressions which correspond in density and dimension with all the particles in the A faces. Only a few very large depressions were observed. There is no definitive explanation for this observation. The lack of complementarity could be caused by the manner in which proteins are intercalated into the membrane (3). Also, when the membrane

FIGURE 3 Cross section through a retinula. The rhabdom (*Rh*) is formed by seven retinula cells (*RC*). They are, in turn, surrounded by pigment cells (*PC*) whose pigment granules were removed partly during the cutting procedure. × 3,500.

FIGURE 4 Thin section through two adjacent layers of orthogonally oriented microvilli. The cross-sectioned microvilli show their hexagonal array. *Inset:* the microvilli are formed by evaginations of the membrane (*Rm*) which give rise to one or several microvilli (arrow). × 20,000; *inset* × 25,000.

FIGURE 5 Cross-fracture through a retinula cell (*RC*) with microvilli (*Mv*) and an adjacent pigment cell (*PC*). In two places (circles), the membrane evaginations branch and give rise to several microvilli. The lower right part of the picture shows the A face of the retinula cell membrane. The microvilli have been broken away, leaving craterlike structures of various diameters. The arrows point to the ridges of the B face of the pigment cell membrane and to ridges of the A face of the retinula cell membrane, respectively. The presence of these ridges indicates that frozen membranes are split in their hydrophobic areas by freeze-fracture. *P* = pigment granules. × 40,000.

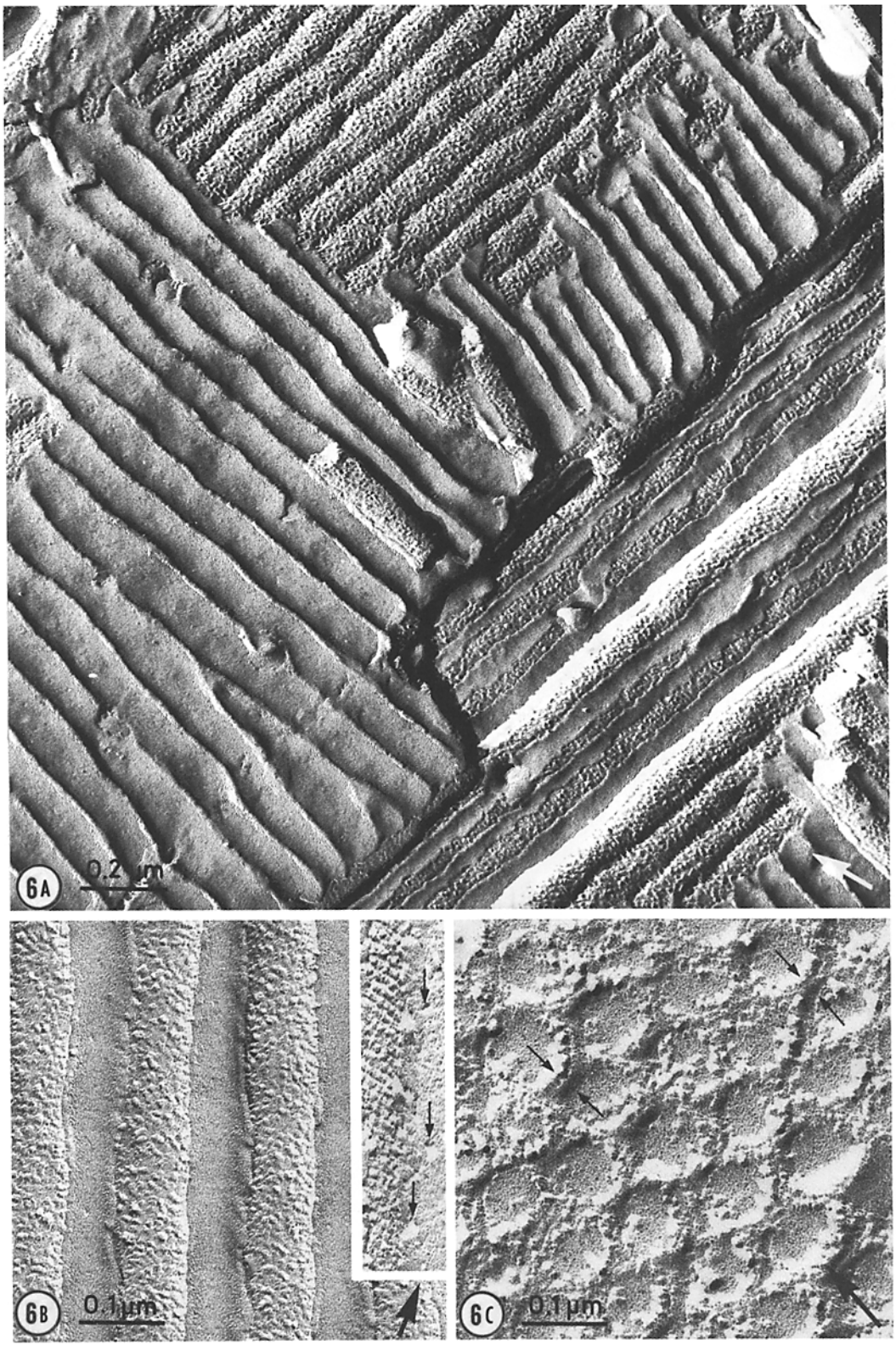
6A
0.2 μm
6B
0.1 μm
6C
0.1 μm

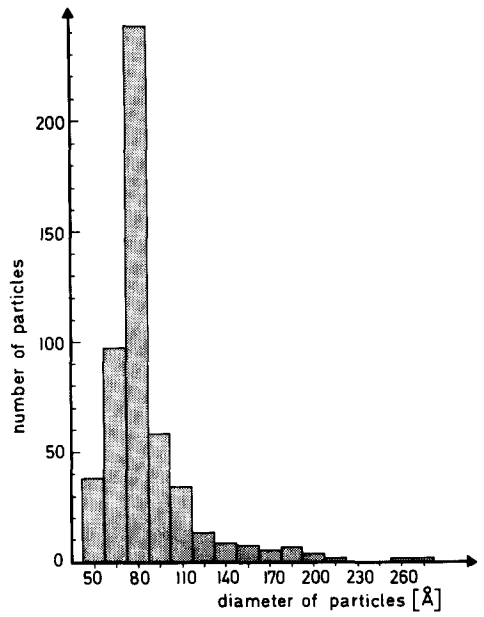

FIGURE 7 Histogram of particle sizes from the A faces of the microvillus membranes. The mean diam is 84 Å. The larger particles may represent aggregates of individual particles.

layers are split apart, the impressions which the particles leave on the B faces might be too small to be resolved or could be filled with the replicating substances. On the other hand, the particles could extend considerably into the outer layer of the membrane but by some recovery process their impressions on the B faces may be rapidly filled by cell membrane constituents. However, the fact that the particles always appear in the A faces suggests that their main attraction is with the inner layer of the membrane, which is similar to the situation known for the particles on disk membranes of vertebrate photoreceptors (6, 21).

Wald (35) extracted two photopigments with the aid of digitonin from rhabdom fractions of *P. clarkii*, with absorbance maxima at 525 and 556 nm, respectively. Similar extraction procedures have yielded photosensitive pigments from rhabdom fractions of other crayfish species (12, 35). Furthermore, Goldsmith and Fernandez[1] have found two photosensitive pigments in the layers of isolated crayfish rhabdoms which seem to have properties similar to those of the visual pigments extracted by Fernandez (12) and Wald (35). The absorbance of a layer with a path length of 20 μm is 0.109 (39). Thus, the total longitudinal absorbance of a rhabdom with a mean path length of 130 μm is about 0.708, when measured with plane polarized light whose e-vector is parallel with the longitudinal axes of all the microvilli. The equivalent absorbance for a random distribution of the molecules in solution is 1.5 times less or 0.472. Assuming a molar absorbance coefficient of 40,500 (4, 5, 30, 37), the combined concentration is 0.896×10^{-3} mol/liter, which is comparable to that found in rod outer segments, 2.5×10^{-3} mol/liter (18, 20).[2] Using the values in Table I, it follows that there are 1.30×10^{-14} mol or $7.82 \times$

[1] Goldsmith, T. H., and H. R. Fernandez. Unpublished observations.

[2] It may seem arbitrary to assign similar absorbance coefficients to both photopigments and to assume them similar to that of vertebrate rhodopsins. However, even though the values might in reality be different, it is very unlikely that the differences are greater than a factor of two. Furthermore, the long wave-length pigment found by Wald (35) in digitonin extracts matches closely the long wave-length limb of the spectral sensitivity curve of dark-adapted eyes and matches the spectral sensitivity curve of blue-adapted eyes even more completely (36). Also, recent intracellular records of the spectral sensitivity of retinula cells (25, 38) further suggest that the 556-nm pigment functions as a visual pigment. The second pigment appears to have no excitatory function and, even though it has linear dichroism (Goldsmith, T. H. and H. R. Fernandez, unpublished observations) similar to that of the 556-nm pigment and bleaches when exposed to light, it is probably a thermally stable photoproduct which coexists with the 556-nm pigment.

FIGURE 6 (A) Freeze-fracture through parts of two adjacent orthogonally oriented layers of microvilli revealing longitudinal profiles to various extents. The smooth B faces of microvilli in the upper layer (left side) as well as the granular A faces of the underlying layer (upper part of picture) are exposed in the plane of their diameters, whereas the alternating A faces and B faces (lower right part of picture) represent incomplete profiles of microvilli. × 68,000. (B) Higher magnification of alternating convex and concave faces of microvilli. The particles of the A faces are randomly distributed. *Inset:* occasionally particles appear to be arranged in rows which are diagonally oriented with respect to the long axis of the microvillus. The arrows point to pits on B faces. × 136,000; *inset* × 136,000. (C) Cross-fractured microvilli showing their hexagonal arrangement. The arrows point to the two layers of the membrane. The particles seem to be associated with the inner layer. × 136,000.

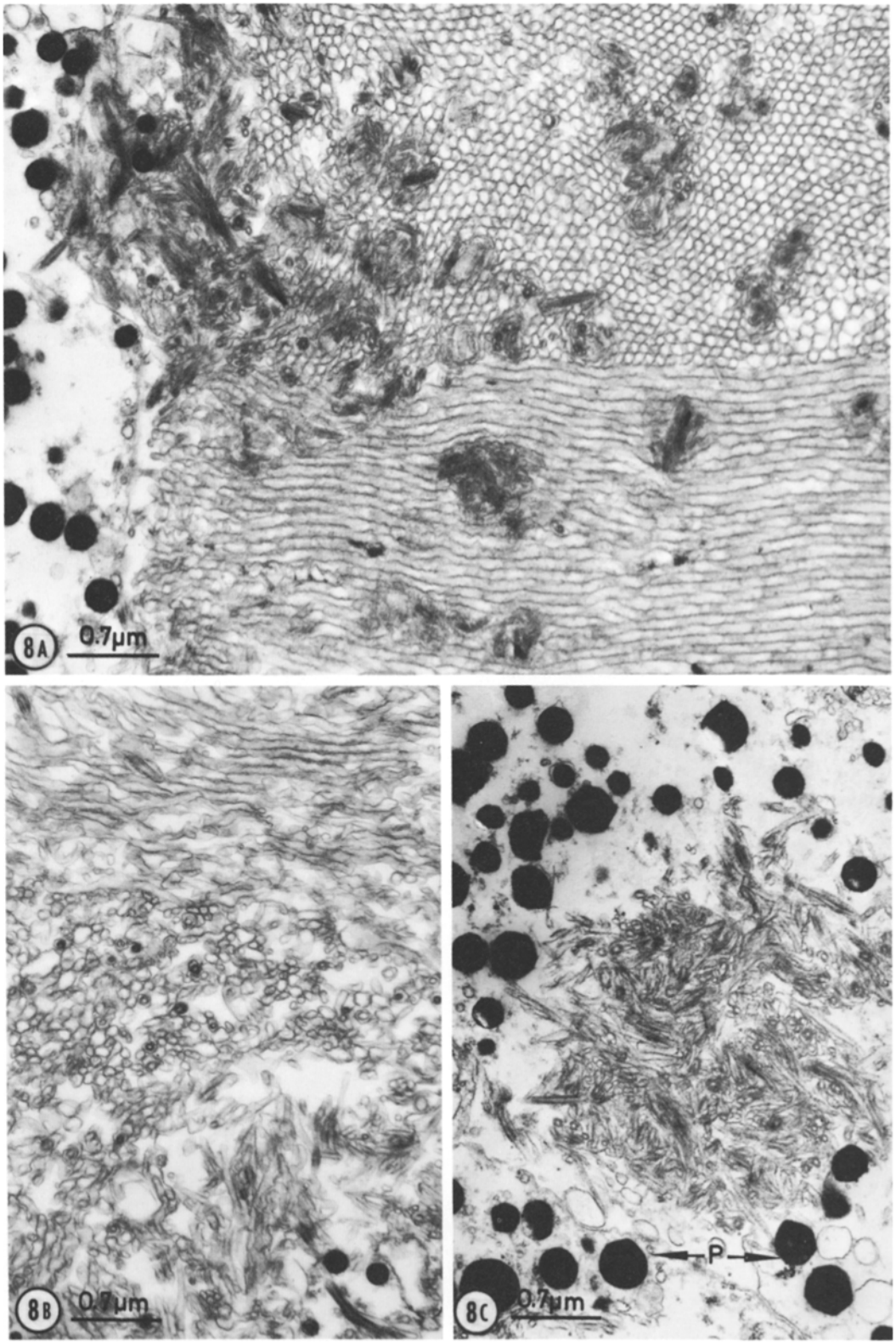

FIGURE 8 Thin sections through rhabdoms after treatment with digitonin. (A) The microvilli begin to break up and form multilayered structures mainly within the rhabdom layers (15 min digitonin). (B) The normal hexagonal arrangement of microvilli is absent (15 min digitonin) (C) Small fragments of microvilli form clusters or lie free in the retinula cell cytoplasm between pigment granules (*P*) (10 min digitonin). × 20,000.

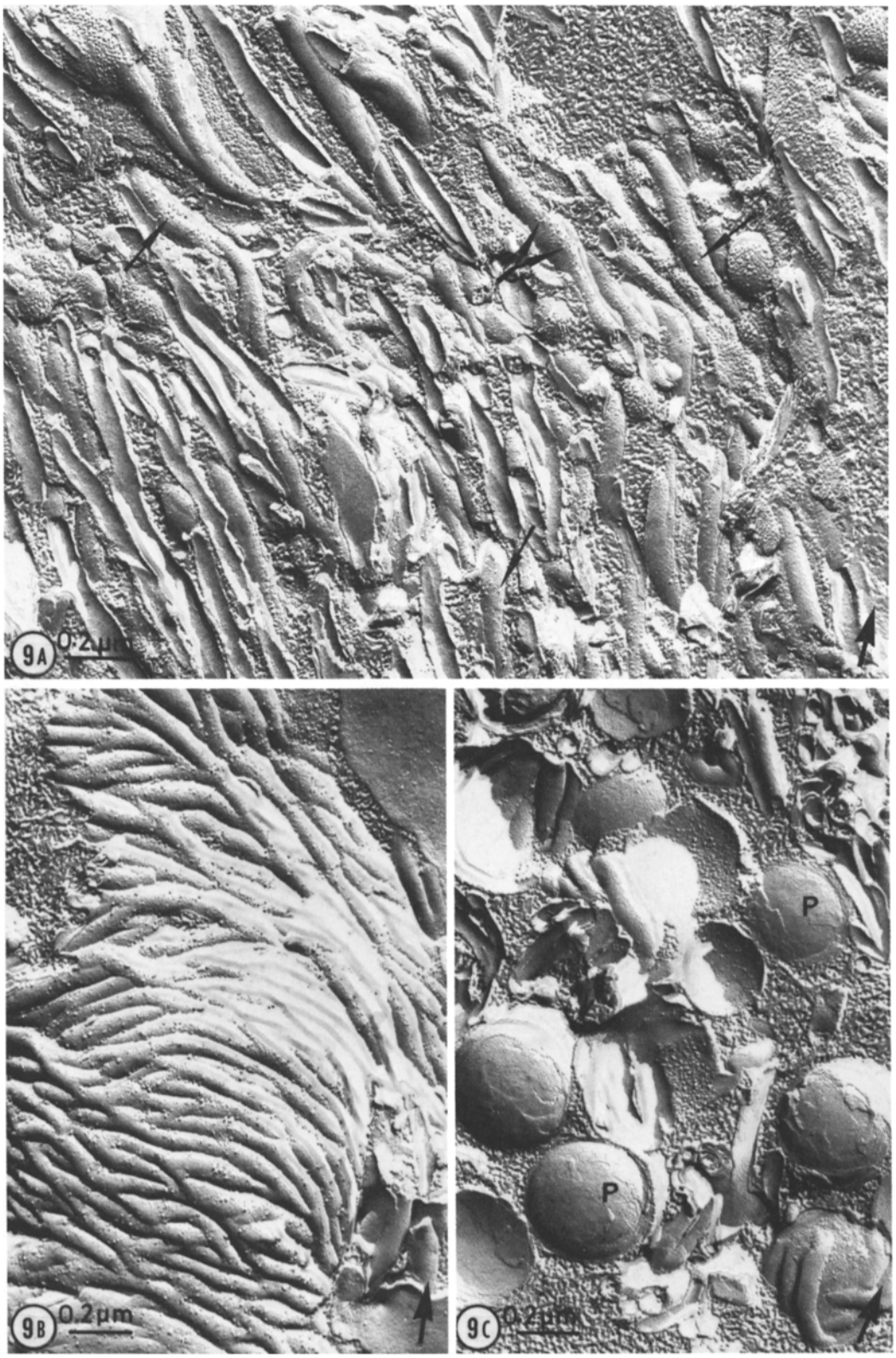

FIGURE 9 Freeze-fractured rhabdoms after digitonin treatment in various stages of disruption. (A) Broken microvilli showing a disorientation of their parallel arrangement (15 min digitonin). Particles are still attached to the A faces of the membrane (arrows). (B) Disrupted microvilli forming clusters in the cytoplasm. A few particles are still associated with the A faces of the membranes (5 min digitonin). (C) The microvilli are broken into small fragments forming aggregates. The membrane profiles appear smooth (15 min digitonin). *P* = pigment grains. × 50,000.

10^9 molecules of photopigment in a rhabdom with a density of 4.03×10^3 molecules/μm^2. By comparison, rod disk membranes have 2×10^4 molecules/μm^2 (1, 7, 21).

Effect of Digitonin

All known visual pigments require agents such as digitonin to extract them from the photoreceptor membranes. This suggests that the molecules are in strong association with the hydrophobic components of the membrane. Digitonin causes marked disruption of the hexagonal arrangement and breakdown of the microvilli into short fragments. Perhaps the most significant effect is that the particles, which are seen in the A faces of untreated microvilli, are gradually removed by digitonin treatment, leaving only smooth membranes. These results are in agreement with recently published observations of the effect of digitonin in vertebrate rod outer segment membranes (21).

If the visual pigments are the main protein component of rhabdom membranes, it seems reasonable to think that the particles in the A faces of freeze-fractured microvilli may represent the photopigment molecules *in situ*. This assumption is supported by the fact that the average number of particles per micrometer^2 is very similar to the estimate of photopigment molecules per micrometer^2 of membrane surface and by the effect of digitonin which removes the particles from the membrane. Furthermore, like those in rod disk membranes, the particles are also associated primarily with the cytoplasmic half of the membrane, and their concentration and density are comparable.

The size of the particles raises one final point. Their mean diameter is almost twice as large as that reported for these particles in vertebrates. This suggests the possibility that their mol wt is larger than 27,000–30,000 (15, 31, 32) reported for vertebrate visual pigments. Analysis of the composition of vertebrate visual pigment shows that it is a complex multimolecular system which consists of opsin, retinal, phospholipids, and carbohydrates (7). At present, information of this nature is lacking for crayfish photoreceptors.

TABLE I

Relevant Dimensional Characteristics of the Rhabdom and Its Constituents

Rhabdom length	130 μm
No. of layers	25
Microvilli per layer	15,500
Total length of microvillus in a layer	20 μm*
Microvillus diameter	0.08 μm
Microvillus membrane thickness	75 Å
Total microvillus membrane area	1.94×10^6 μm^2
Total microvillus membrane volume	1.45×10^{-11} liters

* Since each band consists of two sets of microvilli which meet in the middle of the band, this value represents the combined length of two microvilli.

SUMMARY

The ultrastructure of photoreceptor cells of the crayfish (*P. clarkii*) has been examined by means of thin sections and freeze-fracturing. The study reveals that in the photoreceptor membranes there are particles associated primarily with the A faces of freeze-fracture preparations which have a mean diameter of 80–84 Å and a density of 6,600 per micrometer^2. Treatment of the retina with digitonin (a substance capable of extracting visual photopigments) in Ringer's causes marked disruption of the hexagonal arrangement of the microvilli, breakdown of the microvilli into smaller segments, and gradual removal of the particles. The estimated photopigment concentration in the microvillus is 4,000 per micrometer^2. It is suggested that the observed particles represent the photopigment *in situ*.

We wish to express our appreciation to Professor W. Vogell for his encouragement, support, and helpful suggestions in this work. We also wish to thank Mrs. Ch. Ertl, Mrs. S. Fuchs, and Miss G. Scheck for their valuable technical assistance.

This work was supported by the University of Konstanz and Office of Naval Research Contract N00014-67-A-0269-0013 to Dr. Fernandez.

This paper is dedicated to Professor Dr. Dr. h.c. B. Rensch on the occasion of his 75th birthday.

Received for publication 19 November 1975, and in revised form 26 January 1976.

REFERENCES

1. BLASIE, J. K., and C. R. WORTHINGTON. 1969. Planar liquid-like arrangement of photopigment molecules in frog retinal receptor disk membranes. *J. Mol. Biol.* **39**:417–439.

2. BRANTON, D. 1966. Fracture faces of frozen membranes. *Proc. Natl. Acad. Sci. U. S. A.* **55**:1048–1056.
3. BRANTON, D. 1973. The fracture process of freeze-etching. *In* Freeze-Etching Techniques and Applications. E. L. Benedetti and P. Favard, editors. Société Francaise de Microscopie Electronique, Paris. 107–112.
4. BRIDGES, C. D. B. 1970. Molar absorbance coefficient of rhodopsin. *Nature (Lond.)*. **227**:1258–1259.
5. BRIDGES, C. D. B. 1971. The molar absorbance coefficient of rhodopsin. *Vision Res.* **11**:841–848.
6. CLARK, E. W., and D. BRANTON. 1968. Fracture faces in frozen outer segments from the guinea pig retina. *Z. Zellforsch. Mikrosk. Anat.* **91**:586–603.
7. DAEMEN, F. J. M. 1973. Vertebrate rod outer segment membranes. *Biochim. Biophys. Acta.* **300**:255–288.
8. DEAMER, D. W., and D. BRANTON. 1967. Fracture planes in an ice-bilayer model membrane system. *Science (Wash. D. C.)*. **158**:655–657.
9. EGUCHI, E. 1965. Rhabdom structure and receptor potentials in single crayfish retinular cells. *J. Cell Comp. Physiol.* **66**:411–429.
10. EGUCHI, E., and T. H. WATERMAN. 1966. Fine structure patterns in crustacean rhabdoms. *In* The Functional Organization of the Compound Eye. C. G. Bernhard, editor. Pergamon Press Ltd., Oxford. 105–124.
11. EGUCHI, E., T. H. WATERMAN, and J. AKIYAMA. 1973. Localization of the violet and yellow receptor cells in the crayfish retinula. *J. Gen. Physiol.* **62**:355–374.
12. FERNANDEZ, H. R. 1965. Ph.D. Thesis. A survey of the visual pigments of decapod crustacea of South Florida. University of Miami, Miami, Fla. 133.
13. GOLDSMITH, T. H., and H. R. FERNANDEZ. 1968. Comparative studies of crustacean spectral sensitivity. *Z. Vgl. Physiol.* **60**:156–175.
14. HAMDORF, K., and J. SCHWEMER. 1975. Photoregeneration and the adaptation process in insect photoreceptors. *In* Photoreceptor Optics. A. W. Snyder and R. Menzel, editors. Springer-Verlag KG., Berlin. 263–289.
15. HELLER, J. 1968. Structure of visual pigments. I. Purification, molecular weight, and composition of bovine visual pigment 500. *Biochemistry.* 7:2906–2913.
16. JAN, J. Y., and J. P. REVEL. 1974. Ultrastructural localization of rhodopsin in the vertebrate retina. *J. Cell Biol.* **62**:257–273.
17. KREBS, W. 1972. The fine structure of the retinula of the compound eye of *Astacus fluviatilis*. *Z. Zellforsch. Mikrosk. Anat.* **133**:399–414.
18. LIEBMAN, P. A. 1972. *In situ* microspectrophotometric studies on the pigments of single retinal rods. *Biophys. J.* **2**:161–178.
19. LIEBMAN, P. A. 1975. Birefringence, dichroism and rod outer segment structure. *In* Photoreceptor Optics. A. W. Snyder and R. Menzel, editors. Springer-Verlag KG., Berlin. 199–214.
20. LIEBMAN, P. A., and G. ENTINE. 1964. Sensitive low-light-level microspectrophotometer: detection of photosensitive pigments of retinal rods. *J. Opt. Soc. Am.* **54**:1451–1459.
21. MASON, W. T., R. S. FAGER, and E. W. ABRAHAMSON. 1974. Structural response of vertebrate photoreceptor membranes to light. *Nature (Lond.)*. **247**:188–191.
22. MCNUTT, N. S., and R. S. WEINSTEIN. 1970. The ultrastructure of the nexus: a correlated thin-section and freeze-cleaved study. *J. Cell Biol.* **47**:666–688.
23. MOOR, H., K. MÜHLETHALER, W. WALDNER, and A. FREY-WYSSLING. 1961. A new freezing ultramicrotome. *J. Biophys. Biochem. Cytol.* **10**:1–13.
24. MULLER, K. J. 1973. Photoreceptors in the crayfish compound eye: electrical interactions between cells as related to polarized-light sensitivity. *J. Physiol.* **232**:573–595.
25. NOSAKI, H. 1969. Electrophysiological study of color encoding in the compound eye of crayfish, *Procambarus clarkii*. *Z. Vgl. Physiol.* **64**:318–323.
26. PARKER, G. H. 1895. The retina and optic ganglia in decapods, especially in *Astacus*. *Mitt. Zool. Stn. Neapel.* **12**:1–73.
27. PERRELET, A., H. BAUER, and V. FRYDER, 1972. Fracture faces of an insect rhabdomere. *J. Microsc. (Paris)*. **13**:97–106.
28. PINTO DA SILVA, P. G., and D. BRANTON. 1970. Membrane splitting in freeze-etching. *J. Cell Biol.* **45**:598–605.
29. SHAW, S. R. 1969. Sense-cell structure and interspecies comparisons of polarized-light absorption in arthropod compound-eyes. *Vision Res.* **9**:1031–1040.
30. SHICHI, H. 1970. Spectrum and purity of bovine rhodopsin. *Biochemistry.* **9**:1973–1977.
31. SHICHI, H., M. S. LEWIS, F. IRRIVERRE, and A. L. STONE. 1969. Biochemistry of visual pigments. 1. Purification and properties of bovine rhodopsin. *J. Biol. Chem.* **244**:529–536.
32. SHIELDS, J. E., E. C. DINOVO, R. A. HENRIKSEN, L. R. KIMBEL, and P. G. MILLAR. 1967. The purification and amino acid composition of bovine rhodopsin. *Biochim. Biophys. Acta.* **147**:238–251.
33. VAN HARREVELD, A. 1936. A physiological solution for fresh-water crustaceans. *Proc. Soc. Exp. Biol. Med.* **34**:428–432.
34. VENABLE, J. H., and R. COGGESHALL. 1965. A simplified lead citrate stain for use in electron microscopy. *J. Cell Biol.* **25**:407–408.
35. WALD, G. 1967. Visual pigments of crayfish. *Nature (Lond.)*. **215**:1131–1133.
36. WALD, G. 1968. Single and multiple visual systems in arthropods. *J. Gen. Physiol.* **51**:125–156.
37. WALD, G., and P. K. BROWN. 1953. The molar extinction of rhodopsin. *J. Gen. Physiol.* **38**:189–200.

38. WATERMAN, T. H., and H. R. FERNANDEZ. 1970. E-vector and wave-length discrimination by retinular cells of the crayfish *Procambarus*. *Z. Vgl. Physiol.* **68**:154–174.

39. WATERMAN, T. H., H. R. FERNANDEZ, and T. H. GOLDSMITH. 1969. Dichroism of photosensitive pigments in rhabdoms of the crayfish *Orconectes*. *J. Gen. Physiol.* **54**:415–432.